ORIGINAL RESEARCH

Targeting DNA Topoisomerase IIα in Retinoblastoma: Implications in EMT and Therapeutic Strategies

Qingquan Wei, Nan Lin, Li Wang

Department of Ophthalmology, Tong Ren Hospital, Shanghai Jiao Tong University School of Medicine, Shanghai, People's Republic of China

Correspondence: Li Wang, Department of Ophthalmology, Tong Ren Hospital, Shanghai Jiao Tong University School of Medicine, 1111 Xianxia West Road, Shanghai, People's Republic of China, Email WL1249@shtrhospital.com

Background: This study investigates the role of DNA topoisomerase IIα (TOP2A) in retinoblastoma (RB), focusing on its involvement in epithelial-mesenchymal transition (EMT) and the potential of TOP2A inhibition as a therapeutic strategy.
Methods: We analyzed TOP2A expression in RB tissues using public gene expression databases (GSE97508, GSE110811, and GSE172170) and conducted functional assays in human RB cell lines (Y79 and WERI-Rb-1) modified to knock down or overexpress TOP2A. Assessments included cell proliferation, migration, invasion, and EMT marker expression via RT-PCR and Western blot. Additionally, we evaluated the effects of TOP2A modulation in subcutaneous and liver metastasis mouse xenograft models.
Results: TOP2A was significantly overexpressed in RB tissues ($p < 0.0001$). In vitro, TOP2A knockdown inhibited RB cell proliferation, migration, and invasion, and reversed EMT marker expression ($p < 0.05$), while TOP2A overexpression enhanced these oncogenic processes. In vivo, TOP2A knockdown or inhibition significantly reduced tumor growth and metastasis in both subcutaneous and liver metastasis models ($p < 0.05$). Combination therapy with TOP2A and EMT inhibitors further enhanced anti-tumor effects, significantly reducing tumor burden and metastatic lesions ($p < 0.01$).
Conclusion: TOP2A is pivotal in RB pathogenesis and progression, primarily by regulating EMT. Its inhibition not only curtails RB cell proliferation and metastasis but also reverses EMT, underscoring its potential as a therapeutic target. This study lays the groundwork for further exploration of TOP2A-targeted therapies in RB.
Keywords: targeting DNA topoisomerase IIα, retinoblastoma, epithelial-mesenchymal transition

Background

Retinoblastoma (RB) stands as the most prevalent intraocular cancer among children, affecting approximately 8000 children each year worldwide.[1] This malignancy poses a significant threat not only to vision but also to life, due to its potential for metastasis.[2] The primary manifestations of RB include leukocoria (white pupil), strabismus, and, in advanced stages, vision loss or blindness. Without timely and effective intervention, RB can progress rapidly, with potential for systemic metastasis that significantly endangers patient survival.[3]

Current therapeutic strategies for RB encompass a spectrum of treatments such as chemotherapy, radiotherapy, local treatments, and enucleation in severe cases.[4,5] Despite advancements in treatment modalities, which have improved survival rates and ocular preservation, the management of RB remains challenging 2020.[6] Chemotherapy, the frontline treatment for RB, is fraught with complications such as drug resistance and severe adverse effects including myelosuppression, nephrotoxicity, and neurotoxicity.[7,8] These challenges underscore the urgent need for novel therapeutic targets and strategies to enhance treatment efficacy and reduce toxicity.

The understanding of RB's molecular pathology has significantly advanced, highlighting the critical role of genetic and epigenetic alterations in tumorigenesis and progression.[9] Among these, the epithelial-mesenchymal transition (EMT) emerges as a pivotal process facilitating tumor metastasis.[10] EMT enables tumor cells to acquire migratory and invasive

capabilities, contributing to the dissemination and establishment of distant metastases.[11] The regulation of EMT involves a complex network of signaling pathways and molecular interactions, among which the aberrant activation of oncogenes plays a central role.[12,13]

Recent studies have identified DNA topoisomerase IIα (TOP2A) as a potential oncogene aberrantly activated in various malignancies, including RB.[13] TOP2A, a critical enzyme involved in DNA replication, transcription, and chromosomal segregation, has been linked to cell proliferation and tumor growth.[14,15] Its overexpression has been correlated with poor prognosis in several cancers, making it a promising target for therapeutic intervention.[16] TOP2A plays a significant role in multiple cancers by affecting the G1/S transition of the cell cycle, especially in RB, where its interaction with ICBP90 is a key mechanism for cell cycle regulation. Additionally, TOP2A indirectly regulates the transcription of EMT-related genes by influencing chromatin structure and DNA topology, thereby promoting the invasion and metastasis of tumor cells.[17,18] Studies have shown that TOP2A enhances the activity of the Wnt signaling pathway by stabilizing β-Catenin, which in turn regulates the expression of EMT markers.[19] The combination of EMT inhibitors and TOP2A inhibitors may inhibit tumor progression and metastasis through multiple mechanisms, providing a new direction for the treatment of RB. However, the specific role of TOP2A in RB, particularly its involvement in EMT and metastasis, remains poorly understood.

Given the pivotal role of TOP2A in cellular proliferation and its potential involvement in EMT, this study aims to delve deeper into the function of TOP2A in RB progression. By elucidating the molecular mechanisms by which TOP2A influences EMT and tumor metastasis, we seek to unveil novel therapeutic targets and strategies, potentially revolutionizing RB treatment paradigms. This research not only aims to contribute to the fundamental understanding of RB pathogenesis but also endeavors to pave the way for targeted therapies that could significantly enhance patient outcomes while minimizing treatment-related morbidities.

Materials and Methods
Cell Lines
Human retinoblastoma cell line Y79, WERI-Rb-1 and were purchased from the FuHeng Cell Center, Shanghai. Human embryonic kidney cell line HEK293T was purchased from the China Cell Bank of the Chinese Academy of Sciences. Y79, WERI-Rb-1 were cultured in complete media containing 20% FBS at 37°C in 5% CO_2. HEK293T was cultured in complete media containing 10% FBS at 37°C in 5% CO_2.

Animals Experiments
Eight-week-old male nude mice (BALB/c nu/nu) were raised under 12h day/night circulation conditions with free access to food and water. Y79 shNC cells or Y79 shTOP2A-1/2 cells (1×10^6) were subcutaneously implanted into the right inguinal fold regions of mice (6 mice per group) to establish subcutaneous tumor models. For liver metastasis model, Y79 cells (1×10^6/100 μL PBS) were directly injected into spleens of nude mice (3 mice per group), as previously described.[20]

Drug-Based Interventions
Previous studies have demonstrated that patients with TOP2A gene amplification derive the greatest benefit from chemotherapy regimens involving doxorubicin and epirubicin.[21] In the present study, we investigated the therapeutic effects of a TOP2A inhibitor and an EMT inhibitor in a mouse model. Specifically, TOP2A inhibitor etoposide (M2326, Abmole) or/and EMT inhibitor-1 (M14926, Abmole) was administered intraperitoneally at 8 mg/kg every 3 days to treat mice. Tumor size and body weight were recorded at regular intervals during the period of the experiment. Subcutaneous tumor volumes were assessed on indicated days by a caliper and calculated using the formula: volume = (Length × Width^2)/2. At the end point of the experiment, the mice were sacrificed using cervical dislocation. The tumors were excised for subsequent analysis. All animal experiments were approved by the Ethics Committee of Tongren Hospital, Shanghai Jiaotong University School of Medicine.

Differential Gene (DEG) Expression Analysis

DEG expression RNAseq data were gathered from the GEO entry GSE97508, GSE110811, GSE172170 (www.ncbi.nlm.nih.gov/geo/). DEG expression analysis was conducted using the edgeR package.

Tissue Microarray (TMA)

Commercial human retinoblastoma TMA was obtained from Taibsbio.CHINA (http://taibsbio.com/default.aspx). The TMA contained 18 cases of retinoblastoma, and 12 adjacent normal eye tissues. Representative tumor areas were microscopically selected on HE stained sections. Tissue cores were punched from the defined regions on the donor block by using 2-mm punch needles and inserted into the receiver block followed by histological sectioning and mounting onto slides.

Immunohistochemistry (IHC)

IHC was performed essentially described previously.[22] Briefly, the paraffin sections were deparaffinized in two changes of xylene and then rehydrated in decreasing concentrations of ethanol. Sodium citrate (0.1 M, pH 6.0) was used to restore antibody activity in a microwave oven for 20 min. Endogenous peroxidase was inactivated by 3% hydrogen peroxide at room temperature (RT) for 10 mins. After three washes in PBS, the tissue sections were blocked for 35 mins at RT. The sections were incubated with primary antibodies overnight at 4 °C and washed in PBS for 10 mins for four times. The corresponding secondary antibodies were incubated with the sections for 35 mins at RT. The sections were washed four times in PBS for 10 mins per time. DAB staining and hematoxylin counterstaining were performed. Photographs were taken using an Olympus microscope (Olympus, Tokyo, Japan). As a negative control, duplicate sections were immunostained without exposure to primary antibodies, which were replaced with PBS. Staining results were evaluated by two pathologists independently.

Quantitative Real-Time Polymerase Chain Reaction (qRT-PCR)

Total RNA was isolated using a TRIzol reagent (Invitrogen, Carlsbad, CA, USA) according to the manufacturer's instructions. RNA concentration and purity were assessed using a NanoDrop spectrophotometer (Thermo Fisher Scientific, USA), and samples with an A260/A280 ratio between 1.8 and 2.0 were used for further analysis. For reverse transcription, 1 μg of total RNA was transcribed into complementary DNA (cDNA) using the PrimeScript RT Reagent Kit (Perfect Real Time) (Takara, USA) following the manufacturer's protocol. The reverse transcription reaction was performed in a total volume of 20 μL, which included 4 μL of 5× PrimeScript Buffer, 1 μL of PrimeScript RT Enzyme Mix, 1 μL of Random Hexamers, and 14 μL of RNA and nuclease-free water. The reaction conditions were as follows: 37°C for 15 minutes, followed by 85°C for 5 seconds to inactivate the enzyme. qRT-PCR was conducted using TB Green Premix Ex Taq II (Takara, USA) in a total reaction volume of 20 μL, consisting of 10 μL of TB Green Premix, 0.8 μL of forward primer (10 μM), 0.8 μL of reverse primer (10 μM), 2 μL of cDNA template, and 6.4 μL of nuclease-free water. The sequences of primers used for mRNA expression analysis are provided in Supplemental Table 1. Amplification was performed on a QuantStudio 6 Flex Real-Time PCR System (Applied Biosystems, USA) under the following cycling conditions: Initial denaturation: 95°C for 30 seconds, 40 cycles: 95°C for 5 seconds, 60°C for 30 seconds. The sequences of primers used for measuring mRNA expression levels are shown in Supplemental Table 1. All measurements were performed in triplicate. β-actin was used as a reference gene to normalize gene expression. The values for relative quantification were calculated using the $2^{-\Delta\Delta Ct}$ method after the threshold cycle.

Western Blotting (WB)

Cells and tissues were lysed using RIPA Lysis Buffer (Beyotime, China). The centrifugation was carried out to extract the total protein, the concentration of which was determined using the BCA Protein Assay Kit. The proteins were fractionated by SDS-PAGE and transferred to nitrocellulose membranes. For protein separation, 20–50 μg of total protein was mixed with 5× SDS-PAGE loading buffer (Beyotime, China) and denatured by boiling at 95°C for 5 minutes. The denatured proteins were then fractionated on a 10% or 12% SDS-PAGE gel, depending on the

molecular weight of the target protein, at 100 V for 90 minutes. Proteins were subsequently transferred to nitrocellulose membranes (Millipore, USA) at 300 mA for 90 minutes using a wet transfer system. Nonspecific binding sites were blocked with 10% skimmed milk in TBST (Beyotime, China) for an hour at RT. Then, the membranes were incubated with primary antibodies on a shaker overnight at 4°C. The membranes were then washed 3 times with TBST for 5 minutes each and incubated with horseradish peroxidase (HRP)-conjugated secondary antibodies (diluted at 1:5000 in 5% skimmed milk in TBST) for 1 hour at RT. Afterward, the membranes were washed again 3 times with TBST for 5 minutes each to remove unbound secondary antibodies. Subsequently, the membrane was reacted with ECL reagent (Beyotime, China) for 5 min and followed with a signal exposure in the dark. Finally, the protein bands were visualized using an Immobilon Western Chemiluminescent HRP substrate (Millipore). Information of the antibodies is listed in Supplemental Table 2.

Cell Viability Assay

A Cell Counting Kit-8 (CCK-8) assay was performed as described previously.[23] Y79-shNC/shTOP2A-1/2 and WERI-Rb-1 - shNC/shTOP2A-1/2 cells (1000 per well) were seeded in a 96-well plate and CCK8 assay was carried out daily over a 5-day course to evaluate cell proliferation. At the end of each culture period, the viable cells were measured according to the manufacturer's protocol. CCK-8 reagent (10 μL) (Abmole, USA) was added to each well and incubated for 1 hour at 37°C. The absorbance at a wavelength of 450 nm was used to estimate the viable cells in each well (Perlong, Beijing, China).

Migration and Invasion Assays

The migration of retinoblastoma Y79 and WERI-Rb-1 cells was assessed using the transwell assay with an insert chamber (8-μm pore size; Corning, NY). Briefly, equal quantities of Y79-shNC/shTOP2A-1/2 and WERI-Rb-1 - shNC/shTOP2A-1/2 cells suspended in 200μL RPMI-1640 medium containing 2% FBS were seeded on the upper chambers, and 300 μL RPMI-1640 medium containing 20% FBS was in the lower chambers. After 24 hours of incubation at 37°C, the cells in lower chambers were collected. The viable cell was detected by CCK-8. Also, the invasion assay was performed using similar methods as mentioned above, except that the chamber membrane was precoated with Matrigel (2.5 μg/μL). The number of cells invading across matrigel was counted.

Statistical Analysis

Statistical analysis was performed using GraphPad Prism 9 software. Each experiment was repeated at least three independent times. Data were shown as mean ± SD or mean ± SEM. Differences among groups were assessed using the Student's t-test or ANOVA test. Statistical significance is displayed as * $P < 0.05$, ** $P < 0.01$, *** $P < 0.001$, **** $P < 0.0001$.

Results

TOP2A Is Highly Expressed in Retinoblastoma Tissues

Immunohistochemistry (IHC) analysis demonstrated a significant overexpression of TOP2A in retinoblastoma (RB) tissues compared to normal adjacent tissues. Representative IHC images show intense TOP2A staining in RB tissues (Figure 1A). Quantitative analysis of IHC staining revealed markedly higher levels of TOP2A in RB tissues (Figure 1B). Furthermore, the expression of TOP2A was found to increase progressively with the advancing stages of RB, indicating a potential role in disease progression (Figure 1C). Heatmap analysis of differentially expressed genes (DEGs) from GSE97508, GSE110811, and GSE172170 datasets confirmed the upregulation of TOP2A in RB samples (Figure 1D). Western blot (WB) analysis corroborated these findings, showing elevated TOP2A and NDC80 protein levels in RB cell lines (WERI-Rb-1 and Y79) compared to the non-tumorigenic ARPE-19 cell line. However, there is no significant difference in IL-18 at the cellular level (Figure 1E).

TOP2A Promotes Retinoblastoma Progression Through the EMT Pathway

To elucidate the role of TOP2A in RB progression, we investigated its effect on epithelial-mesenchymal transition (EMT). WB analysis confirmed successful knockdown of TOP2A in Y79 and WERI-Rb-1 cells (Figure 2A). TOP2A
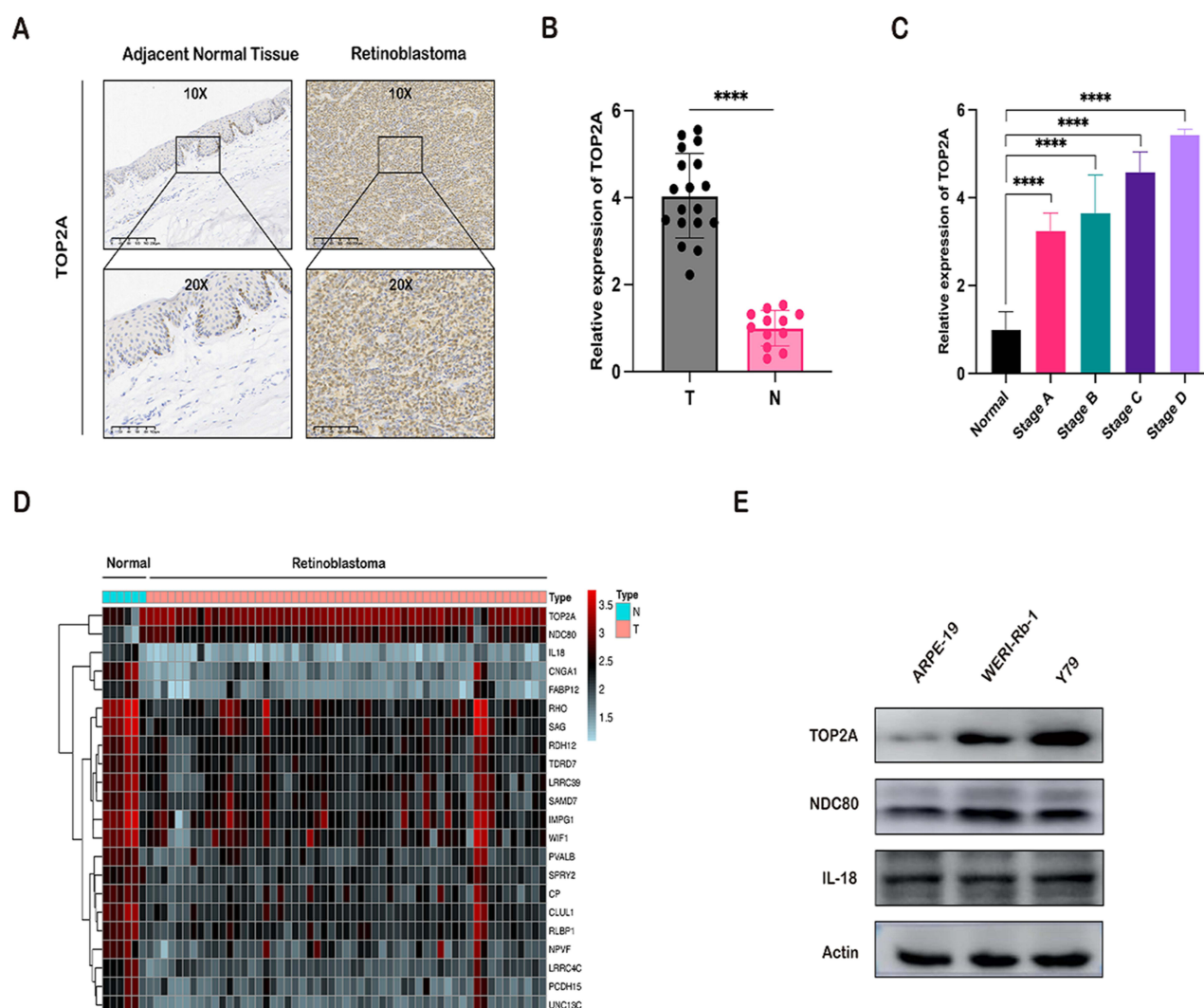
Figure 1 TOP2A is highly expressed in retinoblastoma tissues. (**A**) Representative IHC images of TOP2A staining in tissues from RB patients. (**B**) Quantification of TOP2A IHC staining in tissues from RB patients. (**C**) Expression levels of TOP2A in different stages of RB patients. (**D**) Heatmap of differentially expressed genes (DEGs) in GSE97508, GSE110811, and GSE172170. Red represents the relative upregulation of gene expression; blue represents the relative downregulation of gene expression; black represents no significant change in gene expression. (**E**) WB analysis of TOP2A in ARPE-19, WERI-Rb-1, and Y79 cell lines. (**F**) Quantification of TOP2A expression in ARPE-19, WERI-Rb-1, and Y79 cell lines. **** $P< 0.0001$.

knockdown significantly inhibited cell proliferation in both Y79 and WERI-Rb-1 cells, as demonstrated by cell proliferation assays (Figure 2B). Transwell assays showed that TOP2A knockdown markedly reduced the migratory and invasive capabilities of these RB cells (Figure 2C). RT-PCR analysis revealed that TOP2A knockdown resulted in decreased expression of mesenchymal markers (N-cadherin, Vimentin) and increased expression of the epithelial marker E-cadherin, indicating a reversal of the EMT process (Figure 2D). WB analysis further confirmed these changes in EMT marker expression (Figure 2E).

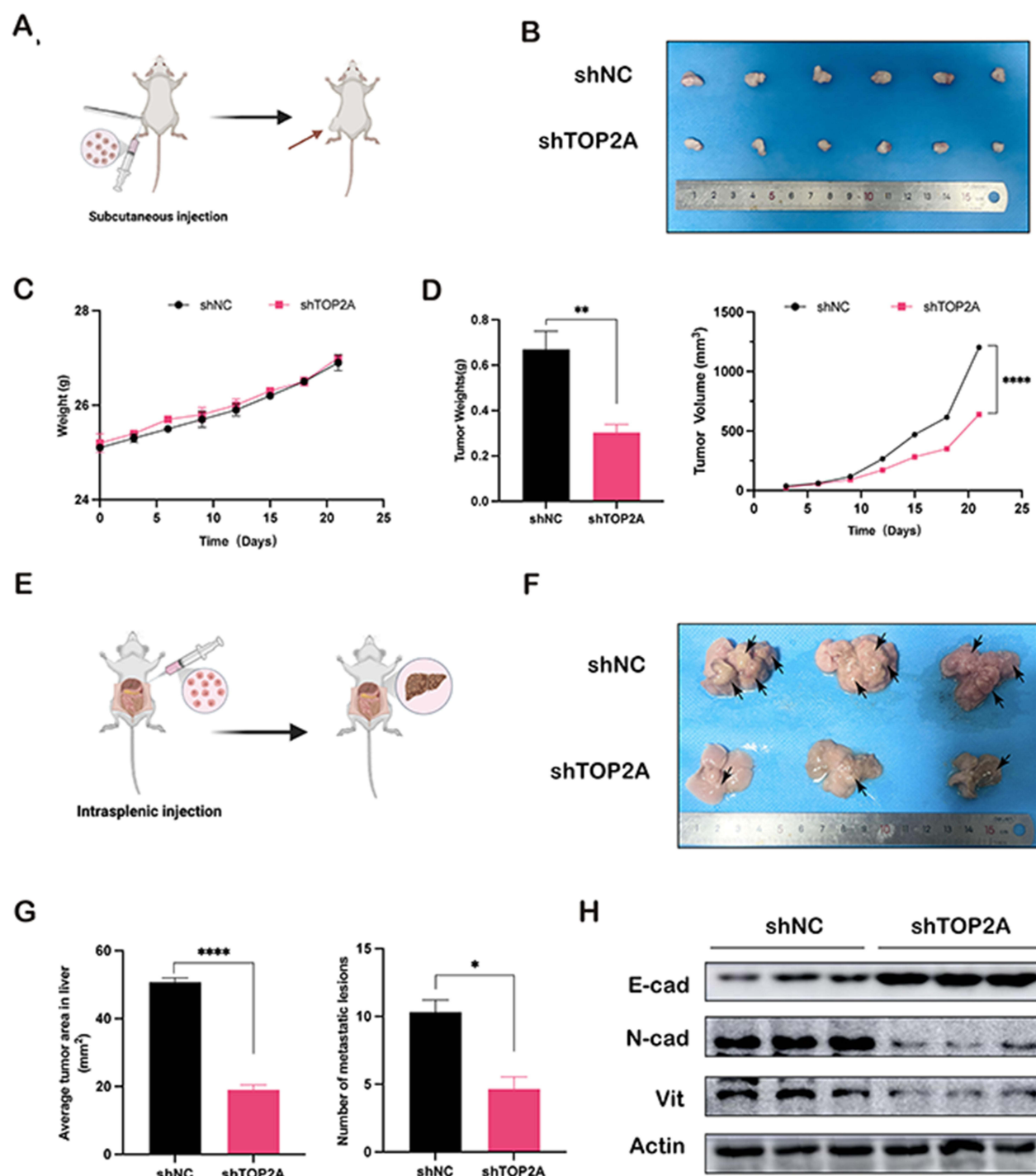## TOP2A Promotes Retinoblastoma Growth and Metastasis in vivo

In vivo studies using subcutaneous xenograft models demonstrated that TOP2A knockdown significantly suppressed tumor growth. The schematic diagram of the subcutaneous xenograft tumor model is shown in Figure 3A. Gross examination of subcutaneous tumors indicated smaller tumor sizes in the TOP2A knockdown group (Figure 3B). The body weights of mice remained stable across different groups (Figure 3C). Tumor weight and volume measurements confirmed a significant reduction in tumor burden in the TOP2A knockdown group compared to controls (Figure 3D).
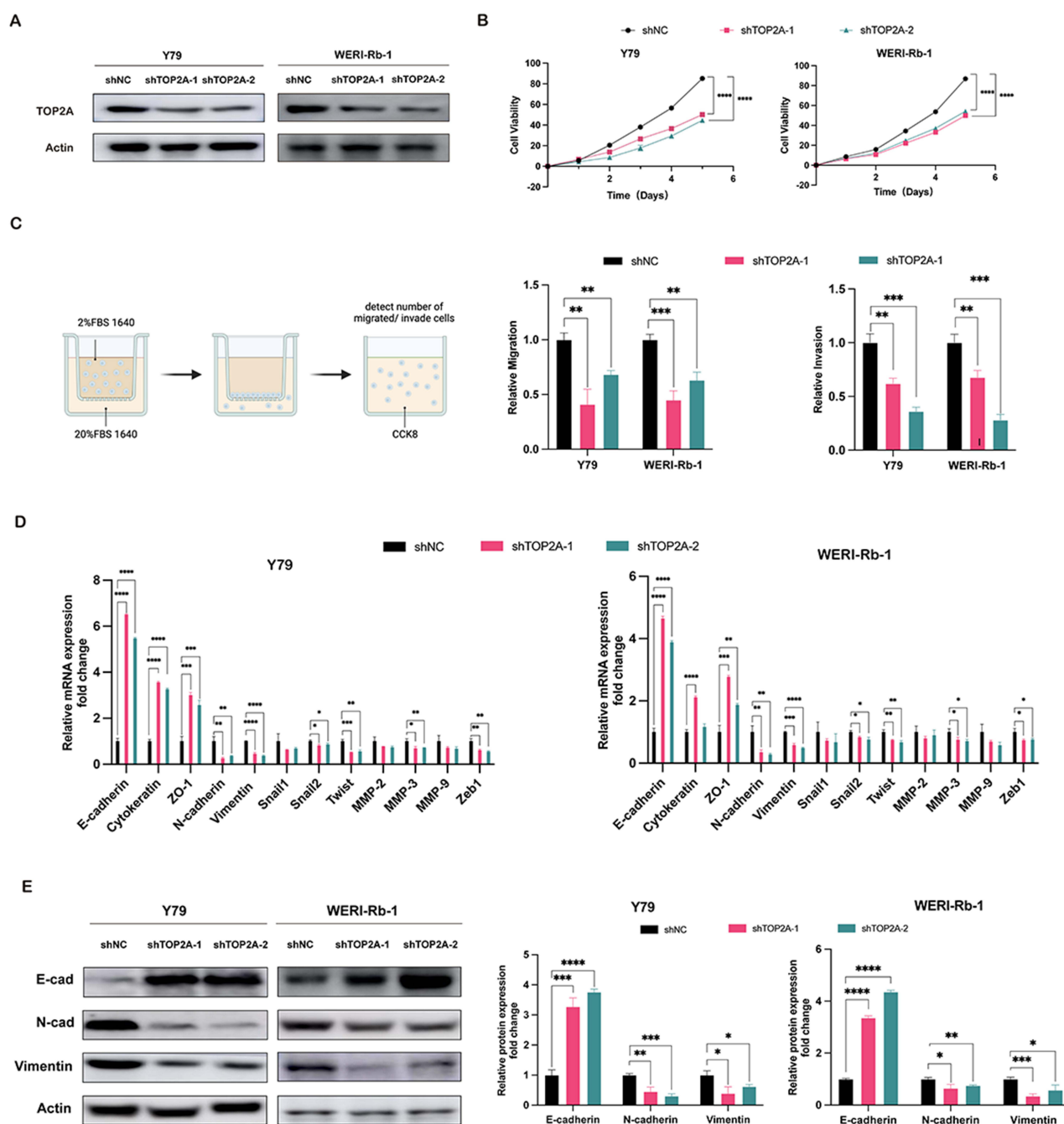
Figure 2 TOP2A promotes retinoblastoma progression through the EMT pathway. (**A**) WB analysis of TOP2A in Y79-shNC/shTOP2A and WERI-Rb-1-shNC/shTOP2A cells. (**B**) Cell proliferation of Y79-shNC/shTOP2A and WERI-Rb-1-shNC/shTOP2A cells. (**C**) Transwell migration/invasion assay to analyze the ability of Y79-shNC /shTOP2A and WERI-Rb-1-shNC/shTOP2A cell migration and invasion. (**D**) RT-PCR analysis of EMT-related genes in Y79-shNC/shTOP2A and WERI-Rb-1-shNC/shTOP2A cells. (**E**) WB analysis of E-cad, N-cad, and Vimentin in Y79-shNC/shTOP2A and WERI-Rb-1-shNC/shTOP2A cells. * $P < 0.05$, ** $P < 0.01$, *** $P < 0.001$, **** $P < 0.0001$.

In the liver metastasis model, TOP2A knockdown led to a significant decrease in metastatic tumor burden, as illustrated by gross images and histopathological examination of liver metastases (Figure 3E and F) and quantification of metastatic tumor area and number of metastatic lesions (Figure 3G). WB analysis of liver metastases showed decreased expression of mesenchymal markers and increased expression of the epithelial marker E-cadherin in the TOP2A knockdown group (Figure 3H).

Figure 3 TOP2A promotes retinoblastoma growth and metastasis in vivo. (**A**) Schematic diagram of subcutaneous xenograft tumor model (n=6 per group). (**B**) Gross picture of subcutaneous tumors originating from Y79-shNC/shTOP2A cells (n=6 per group). (**C**) The body weights of each group change with time (n=6 per group). (**D**) Tumor weight (left) and tumor volume (right) in different groups (n=6 per group). (**E**) Schematic diagram of RB liver metastasis model (n=3 per group). (**F**) Hematoxylin and eosin (H&E) stained sections of liver metastases originating from Y79-shNC/shTOP2A cells (n=3 per group). (**G**) Quantification of metastatic tumor burden in livers via average tumor area and metastatic lesions (n=3 per group). (**H**) WB analysis of E-cad, N-cad, and Vimentin in liver metastases originating from Y79-shNC/shTOP2A cells (n=3 per group). * $P < 0.05$, ** $P < 0.01$, **** $P < 0.0001$.

Intervention in EMT Enhanced Anti-Tumor Effects of TOP2A Inhibitor

Combining EMT inhibition with TOP2A inhibition significantly enhanced the anti-tumor effects in RB. Gross images of subcutaneous tumors from different treatment groups showed smaller tumors in the combination treatment group
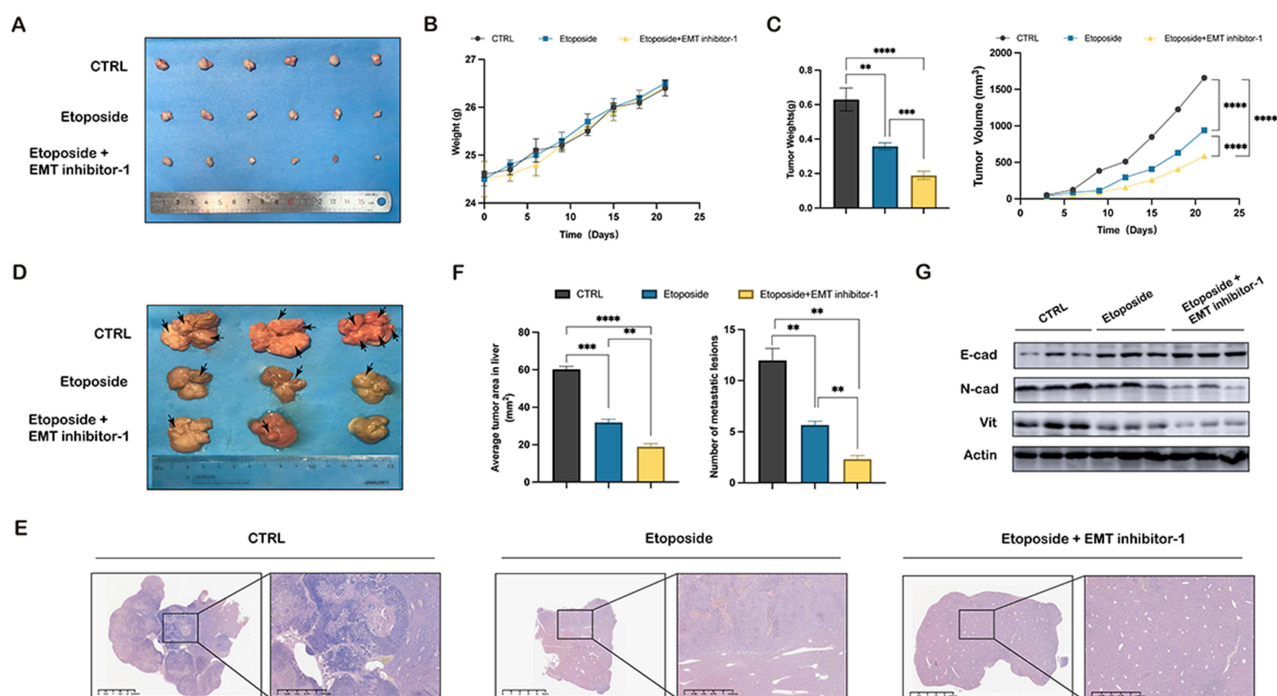
Figure 4 Intervention in EMT enhanced anti-tumor effects of TOP2A inhibitor. (**A**) Gross picture of subcutaneous tumors in each of the different treatment groups (n=6 per group). (**B**) The body weights of each group change with time (n=6 per group). (**C**) Tumor weight (left) and tumor volume (right) in different groups (n=6 per group). (**D**) Gross picture of liver metastases in each of the different treatment groups (n=3 per group). (**E**) H&E stained sections of liver metastases in each of the different treatment groups (n=3 per group). (**F**) Quantification of metastatic tumor burden in livers via average tumor area and metastatic lesions (n=3 per group). (**G**) WB analysis of E-cad, N-cad, and Vimentin in liver metastases from different groups (n=3 per group). ** $P < 0.01$, *** $P < 0.001$, **** $P < 0.0001$.

(Figure 4A). The body weights of mice remained consistent across treatment groups (Figure 4B). Tumor weight and volume measurements indicated that the combination of TOP2A inhibitor and EMT inhibitor resulted in the most significant reduction in tumor burden (Figure 4C).

In the liver metastasis model, combination therapy significantly reduced metastatic tumor burden, as evidenced by gross images and histopathological examination of liver metastases (Figure 4D and E) and quantification of metastatic tumor area and number of metastatic lesions (Figure 4F). WB analysis of liver metastases confirmed decreased expression of mesenchymal markers and increased expression of the epithelial marker E-cadherin in the combination treatment group (Figure 4G).

These results collectively suggest that TOP2A plays a critical role in the pathogenesis and progression of retinoblastoma by promoting EMT. Targeting TOP2A, particularly in combination with EMT inhibitors, represents a promising therapeutic strategy for RB.

Discussion

This study provides substantial evidence of TOP2A's pivotal role in RB progression. The overexpression of TOP2A in RB tissues and its correlation with enhanced tumor aggressiveness align with its recognized function in various cancers.[17,24] Our findings are consistent with previous research highlighting TOP2A's involvement in cell proliferation, migration, invasion, and the EMT process across malignancies.[25,26] Notably, the observed modulation of EMT markers upon TOP2A knockdown or overexpression in RB cells provides new insights into the molecular mechanisms by which TOP2A may influence tumor metastasis.[21]

The role of TOP2A in cancer has been extensively studied; however, its specific impact on RB had not been fully elucidated until now. Previous studies have linked TOP2A overexpression with poor prognosis in cancers such as breast and colorectal cancer, mirroring our observations in RB.[27–29] Our results further expand on these findings by

demonstrating the effectiveness of TOP2A inhibition in reducing RB tumor growth and metastasis in vivo, suggesting that TOP2A's function is not merely prognostic but also directly contributes to tumor pathology.

While this study significantly advances our understanding of TOP2A's role in RB, it also opens several avenues for future research. Firstly, our findings align with recent advances in targeting tumor microenvironmental pathways. Smith et al demonstrated that hypoxia-activated pathways potentiate the efficacy of TOP2A-targeted therapies in solid tumors. This supports our observation that dual inhibition of TOP2A and EMT may exploit overlapping mechanisms, such as hypoxia-driven EMT plasticity, to enhance therapeutic outcomes in RB.[30] Our study shows that TOP2A influences RB tumor invasion and metastasis by regulating EMT-related genes. TOP2A overexpression correlates with increased EMT markers (eg, N-cadherin, Vimentin) and decreased E-cadherin, suggesting it acts upstream by affecting chromatin structure and DNA topology. This is supported by findings that TCF regulates EMT genes via the Wnt pathway. Our work provides a theoretical basis for targeting TOP2A and EMT pathways to suppress RB progression and metastasis, offering new treatment directions.[31] Secondly, the potential for developing TOP2A inhibitors as part of combination therapy for RB should be explored, considering the complex nature of cancer treatment. Finally, studies assessing the role of TOP2A in RB patient samples could provide insights into its clinical relevance and prognostic value.[29]

The identification of TOP2A as a key player in RB progression has significant clinical implications. Given the challenges associated with treating metastatic RB, including the risk of toxicity and the development of resistance to conventional therapies, TOP2A presents a promising therapeutic target.[15,27,32] We are extremely grateful for the reviewer's insightful comments. Research indicates that the zebrafish model is capable of replicating the metastatic pathways observed in human RB, particularly the dissemination through the optic nerve and brain ventricles. Additionally, the zebrafish model's high-throughput capacity and cost-effectiveness render it an optimal choice for both drug screening and mechanistic investigations. Moving forward, this model can be harnessed to dynamically track the migratory patterns of tumor cells, thereby offering novel insights into the metastatic mechanisms underlying RB. This approach will facilitate a more in-depth exploration of TOP2A's role in tumor progression and bolster the theoretical underpinnings for devising innovative treatment strategies.[33] Furthermore, the possibility of using TOP2A expression levels as a prognostic marker could improve patient stratification and treatment planning, enabling more personalized therapeutic approaches.[34–36]

This study is not without limitations. The in vivo experiments were conducted in mouse models, which, while informative, cannot fully replicate the complexity of human RB. Additionally, the potential side effects of systemic TOP2A inhibition require careful consideration, given its role in normal cellular processes. Furthermore, TOP2A inhibitors may exert off-target toxicity on normal proliferating tissues (such as bone marrow and the gastrointestinal tract), necessitating further evaluation of their safety. Moreover, differences in pathophysiology and molecular heterogeneity between mouse models and human RB may impact the clinical translation of the findings. Future research should focus on developing clinical drugs targeting TOP2A and exploring their combined application with other therapeutic strategies.

Conclusion

In conclusion, our study underscores the critical role of TOP2A in the progression of retinoblastoma and highlights its potential as a therapeutic target. By shedding light on the molecular mechanisms underlying RB aggressiveness, this research paves the way for the development of novel treatment strategies, potentially improving outcomes for patients with this challenging disease.

Data Sharing Statement

The original contributions presented in the present study are included in the article material. Further inquiries can be directed to the corresponding authors.

Ethics Approval

The Ethics Committee of Tongren Hospital, Shanghai Jiaotong University approved all animal study procedures.

Acknowledgments

Funding

Disclosure
The authors declare that they have no competing interests in this work.

References

1. Dimaras H, Corson TW, Cobrinik D, et al. Retinoblastoma. *Nat Rev Dis Primers*. 2015;1:15021. doi:10.1038/nrdp.2015.21
2. Global Retinoblastoma Study Group. The Global Retinoblastoma Outcome Study: a prospective, cluster-based analysis of 4064 patients from 149 countries. *Lancet Glob Health*. 2022;10(8):e1128–e1140. doi:10.1016/S2214-109X(22)00250-9
3. Dimaras H, Kimani K, Dimba EA, et al. Retinoblastoma. *Lancet*. 2012;379(9824):1436–1446. doi:10.1016/S0140-6736(11)61137-9
4. Fabian ID, Abdallah E, Abdallah E, et al.; Global Retinoblastoma Study Group. Global retinoblastoma presentation and analysis by national income level. *JAMA Oncol*. 2020;6(5):685–695. doi:10.1001/jamaoncol.2019.6716
5. Munier FL, Beck-Popovic M, Chantada GL, et al. Conservative management of retinoblastoma: challenging orthodoxy without compromising the state of metastatic grace. "Alive, with good vision and no comorbidity". *Prog Retin Eye Res*. 2019;73:100764. doi:10.1016/j.preteyeres.2019.05.005
6. Tomar AS, Finger PT, Gallie B, et al. A multicenter, international collaborative study for American Joint Committee on Cancer staging of retinoblastoma: part I: metastasis-associated mortality. *Ophthalmology*. 2020;127(12):1719–1732. doi:10.1016/j.ophtha.2020.05.050
7. Tomar AS, Finger PT, Gallie B, et al. A multicenter, international collaborative study for American Joint Committee on Cancer staging of retinoblastoma: part II: treatment success and globe salvage. *Ophthalmology*. 2020;127(12):1733–1746. doi:10.1016/j.ophtha.2020.05.051
8. Zhao J, Feng ZX, Wei M, et al. Impact of systemic chemotherapy and delayed enucleation on survival of children with advanced intraocular retinoblastoma. *Ophthalmol Retina*. 2020;4(6):630–639. doi:10.1016/j.oret.2020.02.015
9. Suresh Babu V, Bisht A, Mallipatna A, et al. Enhanced epithelial-to-mesenchymal transition and chemoresistance in advanced retinoblastoma tumors is driven by miR-181a. *Cancers*. 2022;14(20):5124. doi:10.3390/cancers14205124
10. Saxena M, Stephens MA, Pathak H, Rangarajan A. Transcription factors that mediate epithelial-mesenchymal transition lead to multidrug resistance by upregulating ABC transporters. *Cell Death Dis*. 2011;2(7):e179. doi:10.1038/cddis.2011.61
11. Lin S, Gregory RI. MicroRNA biogenesis pathways in cancer. *Nat Rev Cancer*. 2015;15(6):321–333. doi:10.1038/nrc3932
12. Shao XL, Chen Y, Gao L. MiR-200c suppresses the migration of retinoblastoma cells by reversing epithelial mesenchymal transition. *Int J Ophthalmol*. 2017;10(8):1195–1202. doi:10.18240/ijo.2017.08.02
13. Stros M, Polanska E, Struncova S, Pospisilova S. HMGB1 and HMGB2 proteins up-regulate cellular expression of human topoisomerase IIalpha. *Nucleic Acids Res*. 2009;37(7):2070–2086. doi:10.1093/nar/gkp067
14. Vanden Broeck A, Lotz C, Drillien R, Haas L, Bedez C, Lamour V. Structural basis for allosteric regulation of Human Topoisomerase IIalpha. *Nat Commun*. 2021;12(1):2962. doi:10.1038/s41467-021-23136-6
15. Chen Z, Vallega KA, Wang D, et al. DNA topoisomerase II inhibition potentiates osimertinib's therapeutic efficacy in EGFR-mutant non-small cell lung cancer models. *J Clin Invest*. 2024;134(10). doi:10.1172/JCI172716
16. Guturi KKN, Bohgaki M, Bohgaki T, et al. RNF168 and USP10 regulate topoisomerase IIalpha function via opposing effects on its ubiquitylation. *Nat Commun*. 2016;7:12638. doi:10.1038/ncomms12638
17. Bhat UG, Raychaudhuri P, Beck WT. Functional interaction between human topoisomerase IIalpha and retinoblastoma protein. *Proc Natl Acad Sci U S A*. 1999;96(14):7859–7864. doi:10.1073/pnas.96.14.7859
18. Jeanblanc M, Mousli M, Hopfner R, et al. The retinoblastoma gene and its product are targeted by ICBP90: a key mechanism in the G1/S transition during the cell cycle. *Oncogene*. 2005;24(49):7337–7345. doi:10.1038/sj.onc.1208878
19. Lengrand J, Pastushenko I, Vanuytven S, et al. Pharmacological targeting of netrin-1 inhibits EMT in cancer. *Nature*. 2023;620(7973):402–408. doi:10.1038/s41586-023-06372-2
20. Sun R, Lin Z, Wang X, et al. AADAC protects colorectal cancer liver colonization from ferroptosis through SLC7A11-dependent inhibition of lipid peroxidation. *J Exp Clin Cancer Res*. 2022;41(1):284. doi:10.1186/s13046-022-02493-0
21. Tanner M, Jarvinen P, Isola J. Amplification of HER-2/neu and topoisomerase IIalpha in primary and metastatic breast cancer. *Cancer Res*. 2001;61(14):5345–5348.
22. Chen Z, Shao W, Li Y, et al. Inhibition of PCSK9 prevents and alleviates cholesterol gallstones through PPARalpha-mediated CYP7A1 activation. *Metabolism*. 2024;152:155774. doi:10.1016/j.metabol.2023.155774
23. Zhang KL, Zhu WW, Wang SH, et al. Organ-specific cholesterol metabolic aberration fuels liver metastasis of colorectal cancer. *Theranostics*. 2021;11(13):6560–6572. doi:10.7150/thno.55609
24. Turner JG, Dawson J, Sullivan DM. Nuclear export of proteins and drug resistance in cancer. *Biochem Pharmacol*. 2012;83(8):1021–1032. doi:10.1016/j.bcp.2011.12.016
25. Vidal S, Kovacs K, Horvath E, et al. Topoisomerase IIalpha expression in pituitary adenomas and carcinomas: relationship to tumor behavior. *Mod Pathol*. 2002;15(11):1205–1212. doi:10.1097/01.MP.0000036342.73003.55
26. Kwon HB, Park C, Jeon KH, et al. A series of novel terpyridine-skeleton molecule derivants inhibit tumor growth and metastasis by targeting topoisomerases. *J Med Chem*. 2015;58(3):1100–1122. doi:10.1021/jm501023q

27. Liu Y, Yu K, Zhang K, et al. O-GlcNAcylation promotes topoisomerase IIalpha catalytic activity in breast cancer chemoresistance. *EMBO Rep.* 2023;24(7):e56458. doi:10.15252/embr.202256458

28. Press MF, Sauter G, Buyse M, et al. Alteration of topoisomerase II-alpha gene in human breast cancer: association with responsiveness to anthracycline-based chemotherapy. *J Clin Oncol.* 2011;29(7):859–867. doi:10.1200/JCO.2009.27.5644

29. Coss A, Tosetto M, Fox EJ, et al. Increased topoisomerase IIalpha expression in colorectal cancer is associated with advanced disease and chemotherapeutic resistance via inhibition of apoptosis. *Cancer Lett.* 2009;276(2):228–238. doi:10.1016/j.canlet.2008.11.018

30. Smith PJ, McKeown SR, Patterson LH. Targeting DNA topoisomerase IIalpha (TOP2A) in the hypoxic tumour microenvironment using unidirectional hypoxia-activated prodrugs (uHAPs). *IUBMB Life.* 2023;75(1):40–54. doi:10.1002/iub.2619

31. Abraham AD, Esquer H, Zhou Q, et al. Drug design targeting T-cell factor-driven epithelial-mesenchymal transition as a therapeutic strategy for colorectal cancer. *J Med Chem.* 2019;62(22):10182–10203. doi:10.1021/acs.jmedchem.9b01065

32. Elfadadny A, Ragab RF, Hamada R, et al. Natural bioactive compounds-doxorubicin combinations targeting topoisomerase II-alpha: anticancer efficacy and safety. *Toxicol Appl Pharmacol.* 2023;461:116405. doi:10.1016/j.taap.2023.116405

33. Maricic N, Schwermer M, Schramm A, et al. Zebrafish as an orthotopic tumor model for retinoblastoma mimicking routes of human metastasis. *Cancers.* 2022;14(23):5814. doi:10.3390/cancers14235814

34. Schrader C, Meusers P, Brittinger G, et al. Topoisomerase IIalpha expression in mantle cell lymphoma: a marker of cell proliferation and a prognostic factor for clinical outcome. *Leukemia.* 2004;18(7):1200–1206. doi:10.1038/sj.leu.2403387

35. Wilson CS, Medeiros LJ, Lai R, et al. DNA topoisomerase IIalpha in multiple myeloma: a marker of cell proliferation and not drug resistance. *Mod Pathol.* 2001;14(9):886–891. doi:10.1038/modpathol.3880407

36. Chen CC, Gau JP, You JY, et al. Prognostic significance of beta-catenin and topoisomerase IIalpha in de novo acute myeloid leukemia. *Am J Hematol.* 2009;84(2):87–92. doi:10.1002/ajh.21334